EFFECTIVE STRESS ANALYSIS OF PILES IN LIQUEFIABLE SOIL: A CASE STUDY OF A BRIDGE FOUNDATION

Hayden J. Bowen[1] and Misko Cubrinovski[2]

SUMMARY

When evaluating the seismic performance of pile foundations in liquefiable soils, it is critically important to estimate the effects of cyclic ground displacements on the pile response. Advanced analyses based on the effective stress principle account for these effects in great detail by simulating the process of pore pressure build-up and associated stress-strain behaviour of soils. For this reason, the effective stress method has been established as a principal tool for the analysis and assessment of seismic performance of important engineering structures.

In this paper, effective stress analysis is applied to a case study of a bridge pier founded on piles in liquefiable soil. The study examines the likely effects of liquefaction, cyclic ground displacements and soil-structure interaction on the bridge foundation during a strong earthquake. A fully coupled effective stress method of analysis is used to compute the dynamic response of the soil-pile-bridge system. In the analysis, an elastoplastic deformation law based on a state concept interpretation is used for modelling nonlinear behaviour of sand. The seismic performance of the pile foundation is discussed using computed time histories and maximum values of ground and pile displacements, excess pore water pressure and pile bending moments. The advantages of the effective stress analysis are discussed through comparisons with a more conventional pseudo-static analysis of piles.

INTRODUCTION

Soil liquefaction during strong earthquakes results in a nearly complete loss of strength and stiffness in the liquefied soil, and consequent large lateral ground movement. Both cyclic ground displacements and unilateral displacements due to spreading of liquefied soils are very large and damaging to buried lifelines and foundations. Pile foundations embedded in liquefying soils are subjected to two types of lateral loads: kinematic loads due to lateral ground movement, and inertial loads due to vibration of the superstructure. The kinematic loads are distributed along the length of the pile while the inertial loads from the superstructure are transferred to the pile at the pile head. Both loads are oscillatory and with a magnitude that varies significantly over a relatively short period of time during which the soil undergoes a drastic reduction in the effective stress due to rapid build-up of excess pore water pressures and eventual liquefaction.

There are several methods available for analysis of piles in liquefying soils including sophisticated finite element analysis based on the effective stress principle and simplified methods based on the pseudo-static approach. The seismic effective stress analysis essentially aims at a very detailed simulation of the complex soil-pile interaction in liquefying soils through the use of advanced numerical procedures and modelling techniques. This is a step-by-step finite element analysis in which the soil is treated as a two-phase material, with solid and fluid phases. A particular advantage of this approach is that it considers the dynamic response of the entire soil-pile-superstructure system. For this reason and because of its high predictive capacity, this method of analysis is considered as the most appropriate for evaluation of the seismic performance of important structures. The pseudo-static analysis of piles, on the other hand, is a practical engineering approach based on routine calculations and use of relatively simple concepts. Because of its simplicity and reliance on conventional engineering methods, the pseudo-static analysis is particularly suitable for assessment of uncertainties associated with liquefaction through parametric studies. Clearly, the seismic effective stress analysis and the pseudo-static analysis focus on different issues and play complimentary roles in the assessment of pile response in liquefying soils.

The application of the seismic effective stress analysis in the engineering practice is generally constrained by two requirements. Namely, this analysis typically requires detailed information on in-situ conditions, physical properties and deformational behaviour of soils, and it also imposes very high demands on the user regarding the knowledge and understanding of both the phenomena considered and particular features of the adopted numerical procedure. Whereas the latter requirement cannot be relaxed, one should recognize that a different level of rigour could be implemented in the determination of the parameters for the effective stress analysis. In the most rigorous case, the site characterization and parameters of the constitutive model would be determined using detailed field investigations and series of tests on undisturbed soil samples in the laboratory. This kind of detail is rarely affordable, however, and commonly the parameters required for the effective stress analysis are derived based on conventional field tests, existing data on similar soils and well-established empirical correlations. In this paper, the

[1] *Geotechnical Engineer, Tonkin & Taylor Ltd., Christchurch (formerly University of Canterbury, Christchurch (Member).*

[2] *Associate Professor, University of Canterbury, Christchurch (Member).*

latter, less rigorous approach is applied to a case study in Christchurch, in order to:

- demonstrate the applicability of the effective stress analysis to a case study;
- examine the seismic response of the bridge foundation in detail by considering the effects of soil-structure interaction, excess pore water pressure and eventual liquefaction on the response of piles;
- analyse the advantages and disadvantages of performing an advanced analysis over the use of a simplified pseudo-static analysis.

The case study, the Fitzgerald Avenue Bridges in Christchurch, is first described including characteristics of the soil profile and pile foundation. The particular features of the adopted dynamic effective stress analysis are then introduced giving due attention to the development of the numerical model and modelling of the nonlinear behaviour of soil and pile. Next, the computed response of the soil and pile foundation is presented and discussed using time histories of excess pore water pressures, accelerations, displacements and bending moments. Results from the effective stress analysis are eventually compared with corresponding results from a pseudo-static analysis of the piles.

CASE STUDY: FITZGERALD AVENUE BRIDGES

The Fitzgerald Avenue Twin Bridges over the Avon River in Christchurch have been identified as an important lifeline for post-disaster emergency services and recovery operations. To avoid structural failure of the foundations or loss of function of the bridge in an anticipated strong earthquake affecting the Canterbury region, a structural retrofit has been proposed by the Christchurch City Council. In conjunction with bridge widening, this retrofit involves strengthening of the foundation with new large diameter bored piles to be installed. A plan view of the bridge site indicating the location of the new piles with the solid circles is shown in Figure 1. A cross section at the mid span of one of the bridges is shown in Figure 2 where both existing piles and new piles are shown. The existing bridges are supported by piled abutments on the banks and with a central piled pier at the mid-span. According to the initial investigations, the existing piles were founded on potentially liquefiable soils, at about 11 m depth below the ground surface. The new piles will be connected rigidly to the existing foundation and superstructure, and founded into deeper strata consisting of non-liquefiable soils, as shown in Figure 2.

As indicated in Figure 1, field investigations including SPTs and CPTs were conducted at six locations of the bridge site. The results of the field tests showed significant variation in the penetration resistance and thickness of the liquefiable layer estimated using conventional methods for liquefaction assessment. The weakest soil profile was encountered at the northeast corner of the bridge and was therefore given particular attention in this study. Figure 3 summarises the results of two CPT and two SPT measurements at the northeast corner of the bridge including soil stratification. The soil deposit consists of relatively loose sandy soils approximately 15 m thick overlying a denser sand layer. The sandy layers have relatively low fines content predominantly in the range between 3% and 15% by weight. For the purpose of the analysis, the soil profile shown in Figure 3 was further simplified into four layers, as shown in Figure 2, consisting of three, relatively loose, liquefiable sand layers overlying a non-liquefiable base layer of dense sand. The 2 m thick layer at the ground surface has a normalized SPT blow count of N_1 = 10, and overlies a 6.5 m thick layer with N_1 = 15 and a 6.5 m thick layer with N_1 = 10. The base layer is non-liquefiable sand with a normalized SPT blow count of N_1 = 25.

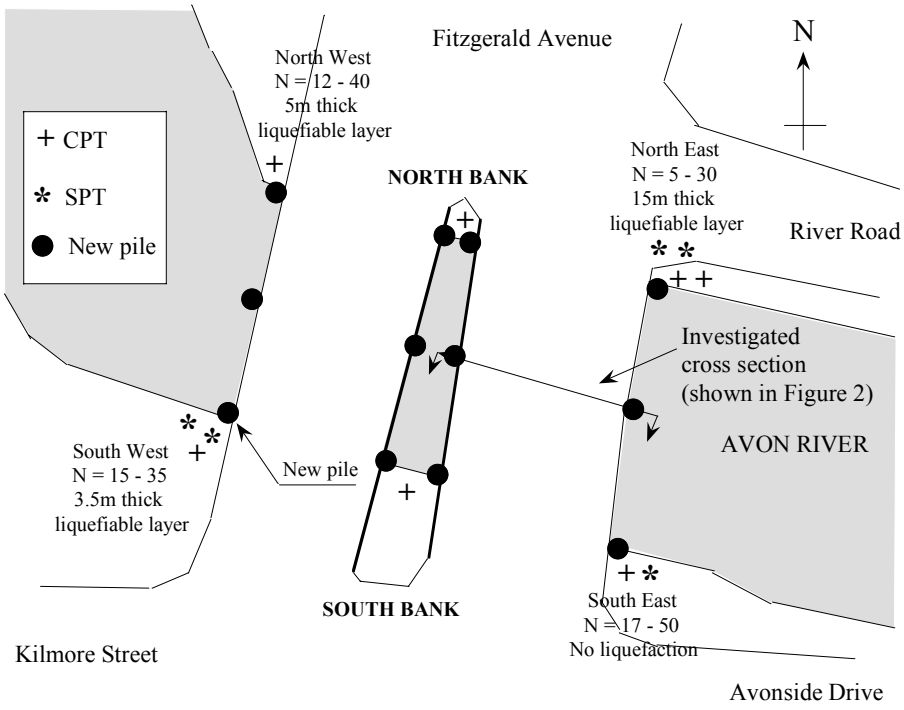

Figure 1. Plan view of the bridge site, showing site investigation locations.

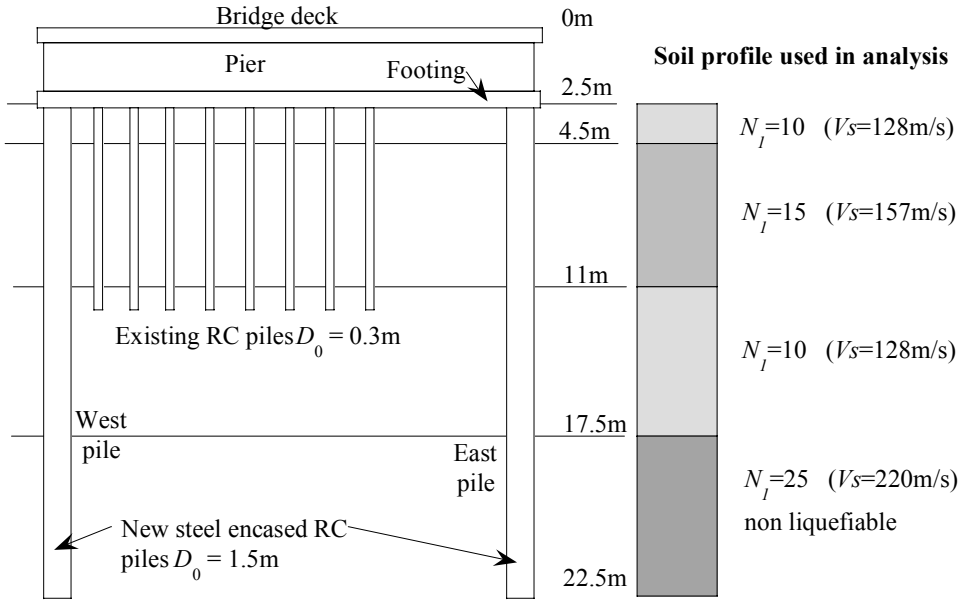

Figure 2. Central pier of bridge: (a) Foundation layout, (b) soil properties used in analysis.

Pile Foundation

The existing bridge pier is founded on eight reinforced concrete piles, 0.3 m in diameter and 9 m long. The proposed retrofit involves installation of bored concrete piles at each end of the extended bridge deck, as shown in Figure 2. The piles are 1.5 m in diameter with a 10mm-thick steel casing. In total, 12 new piles are to be installed for the foundation of the twin bridges at both abutments and at the mid span, as depicted in Figure 1. Tri-linear moment curvature relationships for the new piles (D_o=*1.5 m*) are shown in Figure 4 where the threshold points *C, Y* and *U* denote concrete cracking, yielding of reinforcement and ultimate level or concrete crushing respectively. The moment-curvature relationships for the existing piles were calculated assuming concrete strength in compression of f'_c = 25 MPa and strength of reinforcement bars of f_y = 300 MPa, with an axial load of 150 kN. For the new 1.5 m in diameter piles, a concrete strength of f_c' = 30 MPa, and steel reinforcement at a 0.8% longitudinal reinforcement ratio with a yield strength of f_y = 500 MPa and a 10mm-thick steel casing with f_y = 250 MPa were assumed. Figure 4a shows the tri-linear M-ϕ relationships for the new piles calculated assuming axial loads corresponding to both the serviceability limit state (N =2800 kN) and the ultimate limit state (N=4100 kN). Figure 4b shows the moment curvature relationship for the existing piles, assuming N =150 kN. The axial loads are preliminary estimates only, based on the likely bridge weight and traffic loading.

Earthquake excitation

Previous seismic hazard studies for Christchurch indicate that the most significant contribution to the ground shaking is due to an earthquake on the Porters Pass fault in North Canterbury. Both Howard *et al.* (2005) and Pettinga *et al.* (2001) indicate that the rupture on the strike-slip Porters Pass fault could produce an earthquake of magnitude 7.2 - 7.4. This fault is about 50 km from the site, and probabilistic seismic hazard studies such as Stirling *et al.* (2001) give peak ground acceleration values for Christchurch of 0.37g in a 475 yr event and 0.47g in a 1000 yr event respectively. These attributes of the seismic hazard and strong ground motion characteristics for Christchurch were considered in the selection of the base input motion for the seismic effective stress analysis.

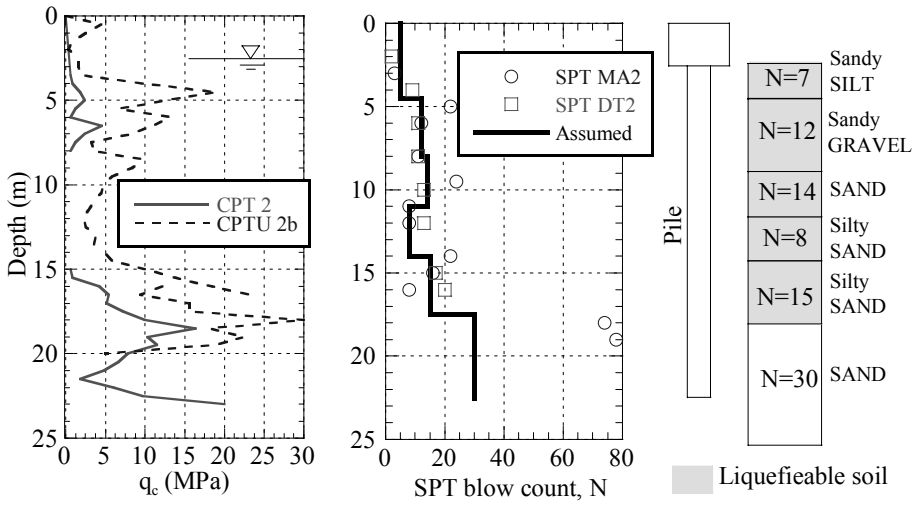

Figure 3. CPT and SPT results for the north – east corner.

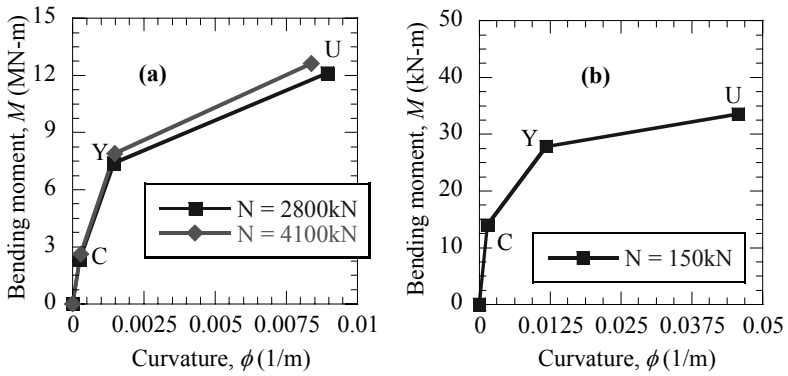

Figure 4. Moment-curvature relationships for (a) new piles (D_0=1.5m) and (b) existing piles.

DYNAMIC ANALYSIS

The seismic effective stress analysis was used to examine in a rigorous manner the response of the strengthened pile foundation during strong ground shaking by considering the complex soil-structure interaction in liquefying soils. To simplify the problem, a two-dimensional plane strain analysis was conducted for a cross section of one of the bridges running through the central pier in the east-west direction. Since the analysis aimed only at the response during the intense ground shaking, it was assumed that the central pier is situated on a level ground. Only a cross section through the east bridge was analysed; the model ignores the effect of the adjacent west bridge on the response. It is considered that the presence of the west bridge will result in a minimal reduction of the liquefaction induced cyclic ground displacements experienced at the east bridge, and this effect has been conservatively ignored. Key considerations here are the inertial effects of the bridge deck and the cyclic ground displacements on the response of the pile foundation. Note that effects of lateral spreading on the pile response were considered separately in a detailed pseudo-static analysis of the piles (Bowen and Cubrinovski, 2007).

The seismic response of the soil-pile-bridge system was evaluated using an advanced dynamic analysis based on the effective stress principle incorporating an elastic-plastic constitutive model specifically designed for modelling soil liquefaction. In the employed numerical method, the soil is treated as a two-phase medium based on the Biot's equations for dynamic behaviour of saturated porous media (Biot, 1956). The so-called *"u-U"* formulation of the equation of motion was used in which the pore-fluid is assumed to be incompressible and the displacements of the solid *(u)* and fluid *(U)* are the unknown variables (Zienkiewicz and Shiomi, 1984). In essence, the method allows for detailed consideration of effects of excess pore water pressure and eventual liquefaction.

A key component in the effective stress analysis is the constitutive soil model, which governs the pore pressure development and associated loss of strength and stiffness in the liquefying soil. In the analysis, an original elastic-plastic constitutive model was employed for modelling sand behaviour (Cubrinovski and Ishihara, 1998a). The so-called Stress-Density Model (S-D Model) utilizes the state concept approach for modelling the combined effects of density and confining stress on stress-strain behaviour of sand (Cubrinovski and Ishihara, 1998b). Consequently, the model can simulate the behaviour of given sand at any density and confining stress by using the same set of material parameters. In other words, it is a true material model unlike most of the conventional soil models that treat each density of a given soil as a different material; typically, the parameters of conventional soil models change with the density of the soil.

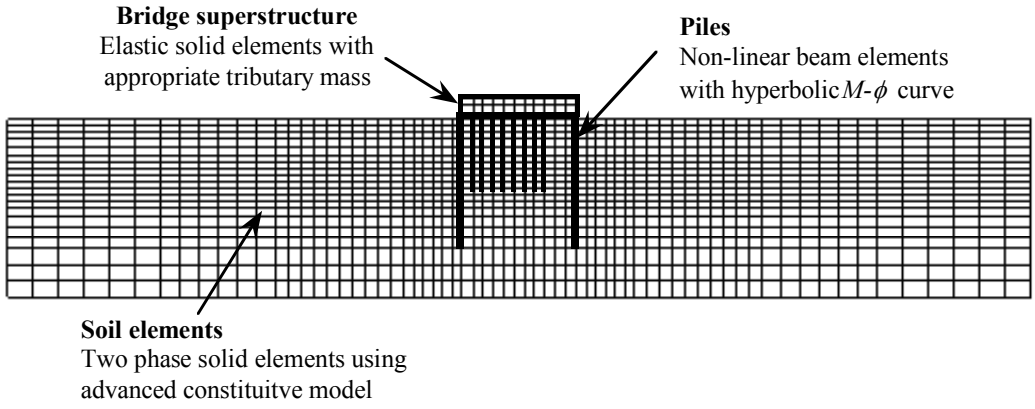

Figure 5. Numerical model used in the analysis.

Key assumptions in the elastic-plastic formulation of the S-D Model are: (i) continuous yielding or vanishing elastic region; (ii) dependence of plastic strain increment direction on the stress increment direction; and (iii) flow formulation allowing for effects due to rotation of principal stresses. The model was specifically tailored for liquefaction problems and has been extensively verified using vertical array records from past earthquakes (Cubrinovski *et al*., 1996; 2000), seismic centrifuge tests (Cubrinovski *et al.,* 1995), large-scale shake table tests on pile foundations (Cubrinovski *et al.,* 1999; 2008) and case histories on damaged piles from the 1995 Kobe earthquake (Cubrinovski *et al.,* 2001). Details of the model can be found in Cubrinovski and Ishihara (1998a; 1998b) while here only the parameters of the model relevant to its application are briefly discussed.

Numerical Model

The 2-D finite element model used in the analysis is shown in Figure 5. The model is 160 m by 30 m in size, with lateral boundaries of the model tied to share identical displacements in order to ensure a free field ground motion near the lateral boundaries. Along the soil-pile interface, the piles and the adjacent soil were connected at the nodes and were forced to share identical displacements, meaning that gapping between the soil and the pile is not allowed in the analysis. Four-node solid elements were employed for modelling the soil and bridge superstructure while beam elements were used for the piles and footing. The footing, bridge deck and pier were all modelled as linear elastic materials with an appropriate tributary mass to simulate inertial effects from the superstructure. The stress-strain behaviour of the soil was modelled using the Stress-Density Model, as described in the following section, whereas the piles were modelled as nonlinear beam members with a moment-curvature relationship approximated by the hyperbolic model. This relationship was determined by fitting a hyperbolic curve to the tri-linear M-ϕ relationship of the pile; the parameters of the hyperbolic model are EI and M_{max} representing the initial bending stiffness and ultimate moment respectively. Figure 6 shows the fitted hyperbolic curve together with the tri-linear M-ϕ relationship of the 1.5 m diameter pile. The initial stiffness and ultimate moment used in the hyperbolic M-ϕ relationships are summarized in Table 1 both for the existing and new piles. Note that the hyperbolic model shown in Figure 6 provides accurate simulation of the actual moment curvature relationship of the pile and that the tri-linear M-ϕ is a typical approximation used in preliminary assessment and design.

The finite-element model shown in Figure 5 was subjected to a base input motion with similar general attributes to those relevant for the seismic hazard of Christchurch. An acceleration record obtained during the 1995 Kobe earthquake (M =7.2) was used as an input motion in the effective stress analysis; this motion was recorded 50 km away from the epicentre in a down-hole array at a depth of 25 m. The motion was scaled to have a peak acceleration of 0.4g, as shown in Figure 7. Needless to say, the adopted input motion is neither representative for the source mechanism nor for the path effects specific to Canterbury, but rather it was considered a relevant input motion that represents the general features of the earthquake event considered in this study. A time step of Δt = 0.005 seconds and Rayleigh damping with parameters α = 0 and β = 0.005 were adopted to ensure numerical stability in the analysis.

Table 1 Parameters of hyperbolic moment-curvature relationships for the existing and new piles

Existing pile, D_0 = 0.3 m		**New pile, D_0 = 1.5 m**	
Initial stiffness EI (MN-m^2)	Ultimate moment, M_u (MN-m)	Initial stiffness EI (MN-m^2)	Ultimate moment, M_u (MN-m)
9.73	0.0337	9347	14.0

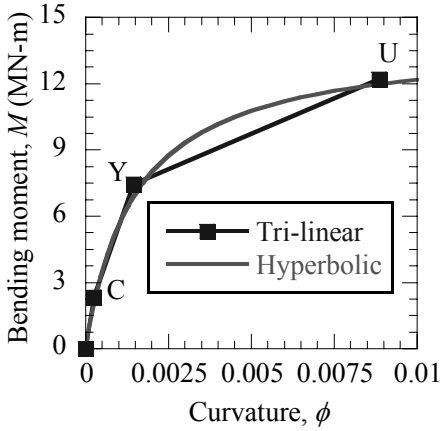

Figure 6. Hyperbolic approximation of the M-ϕ relationship for the new piles.

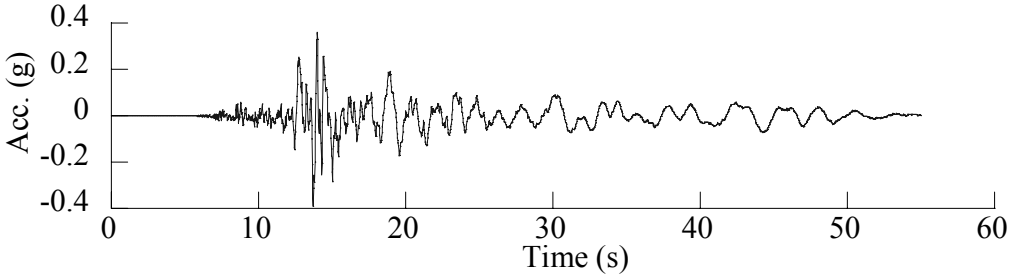

Figure 7. Base input motion used in the effective stress analysis.

Parameters of the soil model

The Stress-Density Model has four groups of parameters, as summarized in Table 2. For a rigorous determination of these parameters, about 15 to 20 laboratory tests are required including monotonic and cyclic, drained and undrained triaxial tests. In the absence of laboratory tests for soils at the Fitzgerald Bridge site, the constitutive model parameters were determined by largely adopting the parameters of Toyoura sand and modifying some of the key parameters as described below. The parameters of Toyoura sand were established based on a previous study (Cubrinovski and Ishihara 1998a; Cubrinovski and Ishihara 1998b) where a comprehensive series of torsional tests was conducted including monotonic drained p'-constant tests, monotonic undrained tests and cyclic undrained or liquefaction tests.

The state parameters and stress-strain parameters of the model are used to define the initial stiffness and peak strength of the stress-strain curve, for any density of the soil and confining stress. The dilatancy parameters essentially control the pore pressure development in the model. These dilatancy parameters, and in particular the parameter S_c, allow precise simulation of the cyclic strength curve or number of cycles required to cause liquefaction. The model is very versatile and allows detailed modelling of various aspects of stress-strain behaviour such as the slope of the liquefaction strength curve or incremental development of strains during cyclic mobility. For the Fitzgerald Bridge analysis, the value of the parameter S_c was determined by simulation of the liquefaction resistance curves shown in Figure 8. The two lines represent the simulated liquefaction resistance curves for the soils with N_1 = 10 and N_1 = 15 respectively. In the simulation process, the S_c value was varied in order to match the target cyclic stress ratio at N_c = 15 cycles shown by the solid symbols in Figure 8. These target cyclic stress ratios were determined using a conventional chart for evaluation of liquefaction resistance based on the SPT blow count, shown in Figure 9 (Youd *et al.* 2001). In this interpretation, the occurrence of liquefaction as plotted with the lines in the CSR vs. $(N_1)_{60}$ diagram in Figure 9 was taken to represent, for a magnitude 7.5 earthquake, the cyclic stress ratio causing liquefaction after 15 uniform cycles of shear stress application. Thus, cyclic stress ratios of 0.17 and 0.23 were calculated for the N_1 = 10 and N_1 = 15 soil layers respectively, assuming a fines content of 10%. Note that both appropriate fines content and magnitude scaling factor have to be used when evaluating the liquefaction resistance based on the empirical chart.

The elastic shear constant, A, is used for calculation of the shear modulus, and in this case was determined by back-calculation in which the elastic shear modulus, G_e, was defined as

$$G_e = \rho \cdot V_s^{\,2} \qquad (1)$$

where ρ is the mass density of the soil and V_s is the shear wave velocity. The adopted values for V_s are summarized in Figure 2. Table 2 shows the soil parameters used in the analysis.

RESULTS

Figure 10 shows the reduction in the mean effective stress caused by the excess pore pressure build-up throughout the model at different times throughout the shaking. In the weaker (N_1 =10) layer the pore water pressure builds up suddenly after the first cycle of strong shaking (t =13.5s); liquefaction starts at the top of the layer and spreads downwards. At t =14.5 seconds the weaker layer has completely liquefied in the free field. The free field behaviour in the stronger (N_1 =15) layer is different; here, the pore water pressure build up is much slower and spreads outwards from the piles. Some stiffening effects from the piles are apparent in the development of the pore pressure in the foundation soil, in-between the piles. The difference in the mean effective stress between t = 23s and t = 55.0s indicates that shallow parts of the deposit may liquefy after the strong shaking due to upward seepage flow and dissipation of excess pore water pressures from the deeper loose sand layer. This set of figures depicts the development process and extent of liquefaction throughout the soil deposit and time.

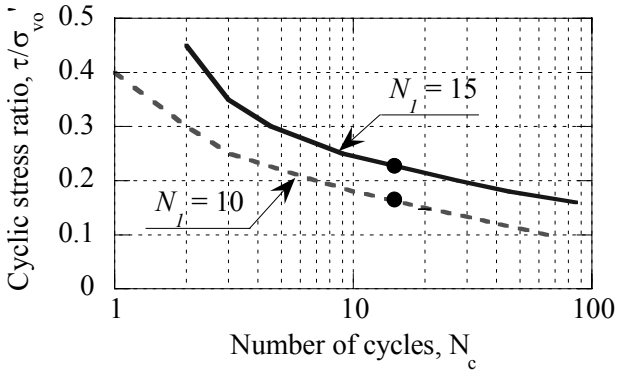

Figure 8. Simulated liquefaction resistance curves for N_1 =10 and N_1 =15 soil layers.

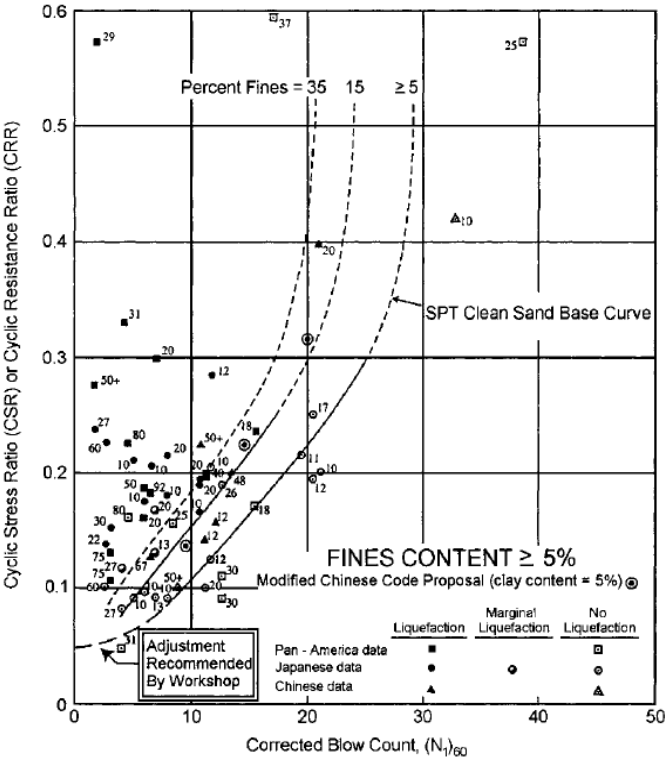

Figure 9. Empirical chart used to evaluate the occurrence of liquefaction using the SPT blow count (Youd et al. 2001).

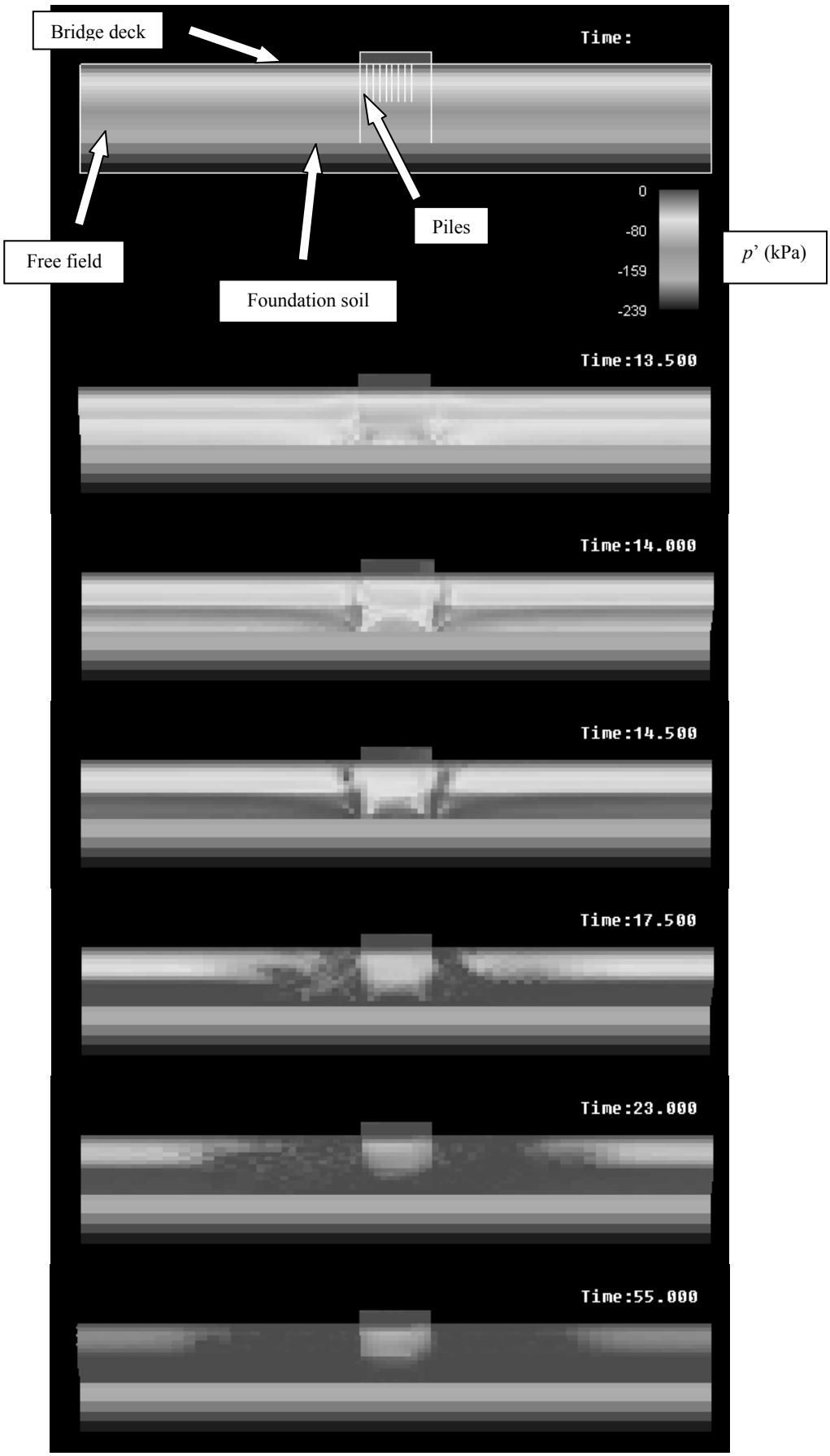

Figure 10. Development of liquefaction throughout the model illustrated by reduction in the mean effective stress p'.

Table 2 Soil model parameters used in analysis

Material parameter	Value
Elastic parameters	
Shear constant, A	250 for N_1 =10, 350 for N_1 =15
Poisson's ratio, ν	0.15
Exponent, n	0.6
State index parameters	
Upper reference line (void ratio, normal stress in kPa)	(0.895, ≤ 400)
Quasi-steady state line	(0.873, 30)
	(0.870, 50)
	(0.860, 100)
	(0.850, 200)
	(0.833, 400)
Stress strain parameters	
Peak stress ratio coefficients a_1 , b_1	0.021, 0.592
Min. shear modulus coefficients a_2 , b_2	13.0, 98.0
Max. shear modulus coefficients a_3 , b_3	55.0, 291.0
Degradation constant, f	4
Dilatancy parameters	
Dilatancy coefficient (small strains), μ_0	0.20
Critical state stress ratio, M	0.60
Dilatancy strain, S_c	0.005

Ground Response

We will first examine the computed ground response in the free field, which is not affected by the presence of the pile foundation. Figure 11a shows computed time histories of excess pore water pressure at two different depths throughout the soil profile in the free field. Here z = 9.5 m and z = 15.7 m depths correspond to the second layer (N_1=*15*) and the third layer (N_1 =*10*) respectively. In the weaker layer (N_1 =10), liquefaction occurs straight after the first cycle of strong shaking, as indicated by the rapid increase in the pore water pressure ratio (u/σ'_v) in Figure 11a. In the stronger layer (N_1 =15), however, the excess pore pressures build up gradually with the application of cyclic shear stresses and liquefaction doesn't fully develop; the pore pressure ratio reaches a value of about 0.88 at the end of the shaking (t = 55 seconds). Note that here a pore pressure ratio of unity indicates complete liquefaction. Figure 11b illustrates the development of the excess pore pressure throughout the depth of the deposit by depicting snapshots of the pore pressure ratio values and hence the extent of liquefaction at different stages of shaking or time sections. This plot shows that the looser sand layer (N_1 =*10*) completely liquefied whereas in the denser sand layer (N_1 =15) the peak pore pressure ratio was in the range between 0.4 and 0.9 at the end of the shaking.

Effects of liquefaction on the ground response are evident in Figure 12 where acceleration time histories at three different depths are shown. Following the complete liquefaction of the mid layer at about 13-14 seconds, the accelerations above the liquefied layer decrease significantly and the ground motion shows loss of high frequencies and elongation of the vibration period. This is a typical post-liquefaction ground response showing increase in displacements and decrease in accelerations due to significant loss of stiffness and "softening" of the liquefied layer. The reduced accelerations and consequent reduction in shear stresses in the ground can explain the slower and gradual build-up of the excess pore water pressure in the layers above the liquefied layer. Clearly, the response of the weaker layer significantly affects and, in this case, practically governs the response of the layers above.

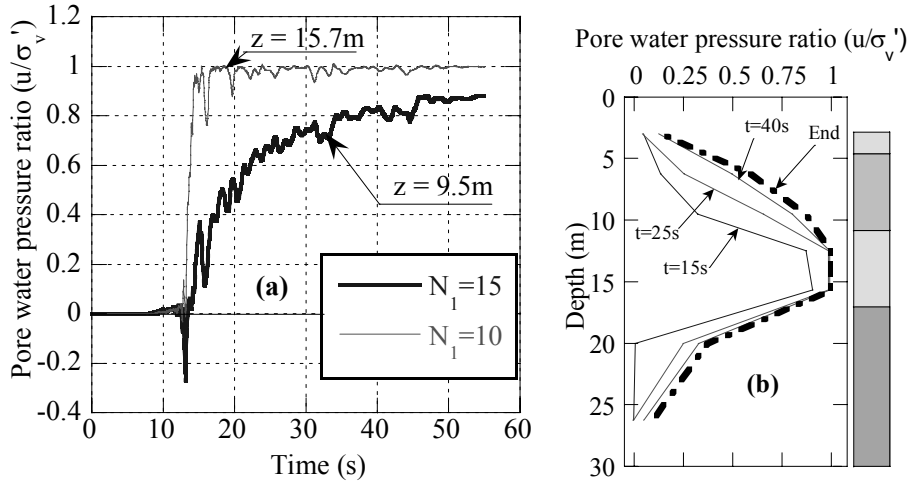

Figure 11. Excess pore water pressures in the free field; (a) time histories showing the development of pore pressure and eventual liquefaction at different depths, (b) distribution of excess pore water pressure ratio throughout the depth of the profile at different times.

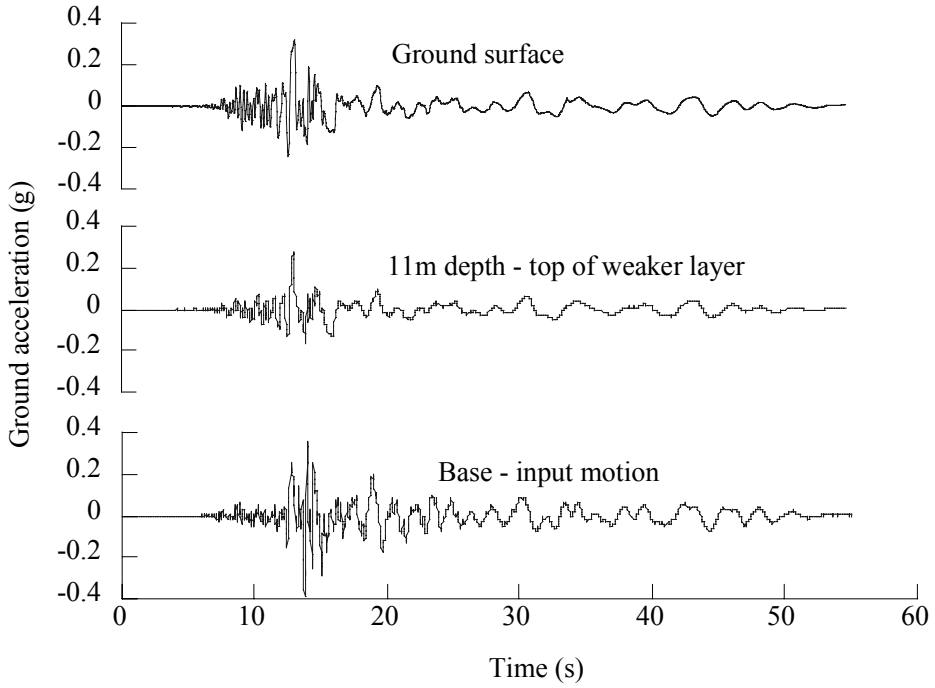

Figure 12. Free field acceleration time histories at different depths of the soil deposit.

The maximum values of the ground acceleration, shear strain and ground displacement, plotted in Figure 13, clearly display the effects of liquefaction on the free field ground response. Figure 13a shows a decrease in acceleration above the weaker layer that liquefied rapidly; this phenomenon has been observed in down-hole array records during past earthquakes (Ishihara and Cubrinovski 2005) and in many shake-table experiments on scaled-down models of relatively loose sands that do not exhibit cyclic mobility (Cubrinovski *et al.,* 2008). Figures 13b and 13c show that the majority of the ground deformation occurs in the mid layer with N_1 =10, where the peak shear strains reach about 4%. The strains in the shallow part of the deposit are well below 1%, which is consistent with the lower excess pore water pressures generated in these layers.

In general terms, the pile foundation provides a stiffening effect to the surrounding foundation soil. This is illustrated in Figure 14, which compares the ground responses in the free field and in the soil between the piles, at 8 m depth. Despite large increases in the pore water pressure, the foundation soil retains some stiffness and shows effects from the interaction with the piles. The stiffening effect of the piles on the response of the foundation soil is more apparent in Figure 15 where time histories of horizontal ground displacements in the foundation soil and free field ground are compared. The peak horizontal displacement in the free field reaches 0.3 m whereas the peak displacement of the foundation soil is less than 0.2 m.

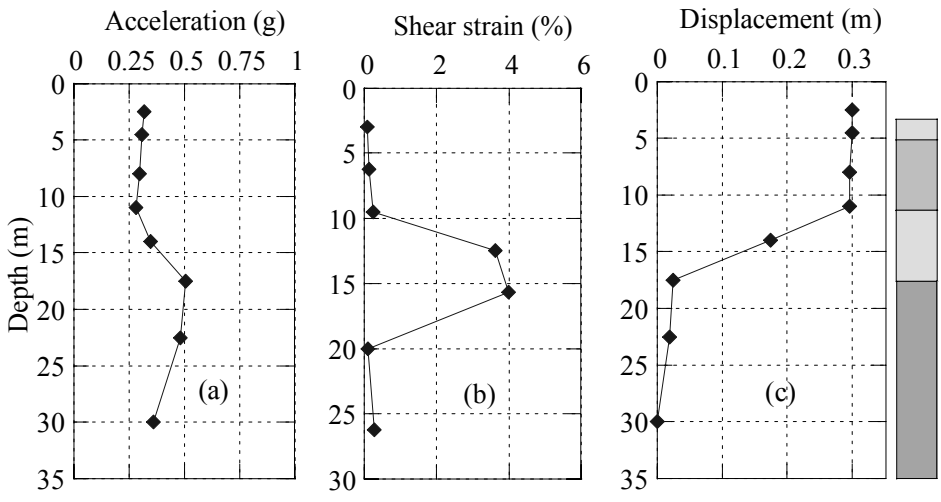

Figure 13. Maximum free field response: (a) accelerations, (b) shear strains, (c) ground displacements.

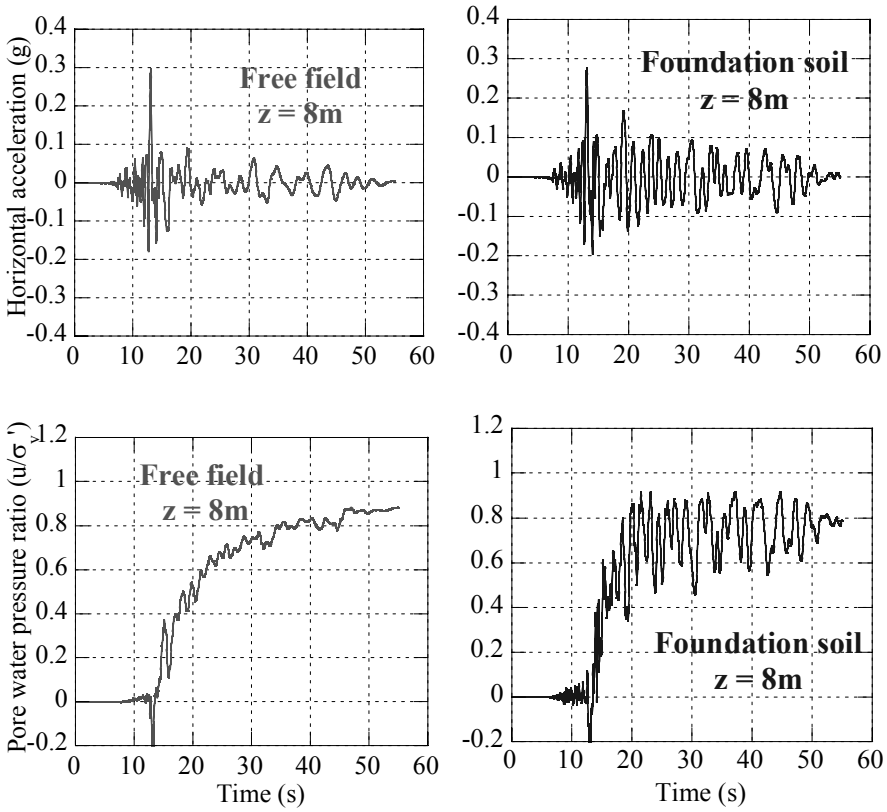

Figure 14. ***Time histories of acceleration and excess pore water pressure in the stronger liquefied soil (N_1=15 at z =8 m) for locations (a) in the free field; and (b) in the foundation soil.***

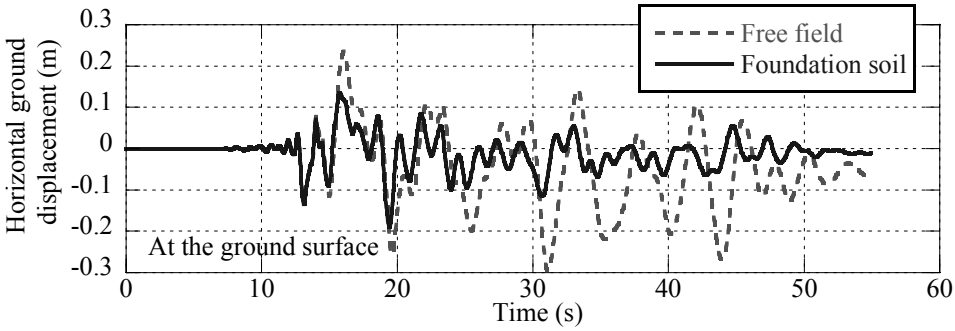

Figure 15. Comparison of the horizontal displacement at the ground surface for locations in the free field and in between the piles.

Pile Response

The modelling of the non-liquefied base layer may significantly affect the pile response especially bending moments or curvatures at the interface between the liquefied layer and underlying base layer. For this reason, three analyses were conducted using different base layer properties; the first analysis used a base layer with a non-linear stress-strain relationship defined by the initial stiffness and shear strength of the base layer. In addition, two analyses were conducted using base layers with equivalent linear stress-strain relationships. In the equivalent linear approach, a degraded secant shear modulus *G* was used to account for the effects of pore pressure build-up and non-linear behaviour of the soil at large strains. In the two analyses, the shear modulus was degraded to 40% and 25% of its initial value respectively. Figure 16 shows stress-strain relationships in the base layer for the three analysis cases, for a free field soil element at a depth of 20 m.

Figure 17a shows the bending moment distribution with depth for the west pile computed in the analysis with a non-linear base layer, plotted for the time when the maximum bending moment was reached at the pile head. The pile exhibits a deformation pattern typical of piles in liquefied soils, with peak bending moments occurring at the pile head and at the interface between the liquefied and underlying base layer. It can be seen that the bending moment exceeds the cracking level in the top 10 m of the pile; the largest moments occur at the pile head but do not exceed the yield moment of the pile. Figure 17b shows the corresponding lateral displacement of the pile at the time of the maximum bending moment together with the maximum horizontal displacement of the ground in the free field. This response indicates that in the top 16 m of the soil deposit, the free field ground displacement is greater than the displacement of the pile and hence over this depth the soil is pushing the pile in the direction of ground movement. Conversely, the soil between 16 m and 20 m depth resists the pile movement, as illustrated schematically in Figure 17c.

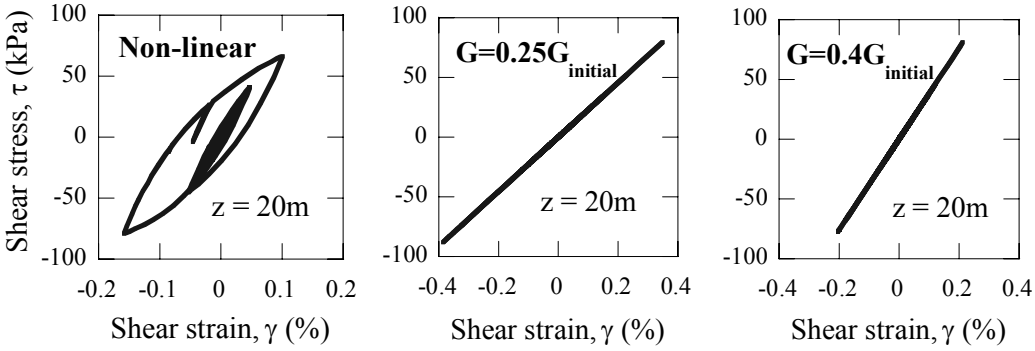

Figure 16. Computed stress-strain relationships in the non-liquefied base layer for three different analyses: non-linear case, equivalent linear case with $G=0.25G_{initual}$ and equivalent linear case with $G=0.4G_{initial}$

A time-history of the bending moment at the pile head is shown in Figure 18. The response shown in Figure 17 corresponds to the peak bending moment attained at about 19 seconds on the time scale. Figure 18 shows that this level of response well above cracking but slightly below yielding was reached three times over the period of intense shaking for the particular input motion used in this study.

Figure 19 shows the computed pile response for the two analyses with an equivalent linear model for the base layer. Both analyses show larger bending moments and displacements of the pile as compared to the analysis with a nonlinear base layer. It can be seen that the stiffness of the base layer particularly affects the bending moment at the interface between the liquefied layer and base layer. A comparison of Figures 17a and 19a shows that the peak bending moment at this interface increases with the stiffness of the base layer. In effect, the relative stiffness between the base layer and overlying liquefied layer controls the bending response at this interface; presuming that the stiffness of the liquefied soil is nearly identical in all three analyses, the above-mentioned relative stiffness is smallest for the nonlinear base layer and highest for the equivalent linear model with $G = 0.4G_{initial}$. This is clearly reflected in the size of the bending moment at the interface for these three analysis cases.

To examine further the cause of these differences, Figure 20 shows the computed response near the pile tip in more detail. It can be seen in this figure that the pile tip displacement is virtually zero for the equivalent linear cases while it is about 7 mm in the case of non-linear base layer. This indicates that the equivalent linear base layer effectively provides a nearly fixed condition at the pile tip; on the other hand, the pile is not sufficiently constrained when a non-linear base layer is used and this is an additional contributor to the smaller bending moments at the interface achieved in this analysis.

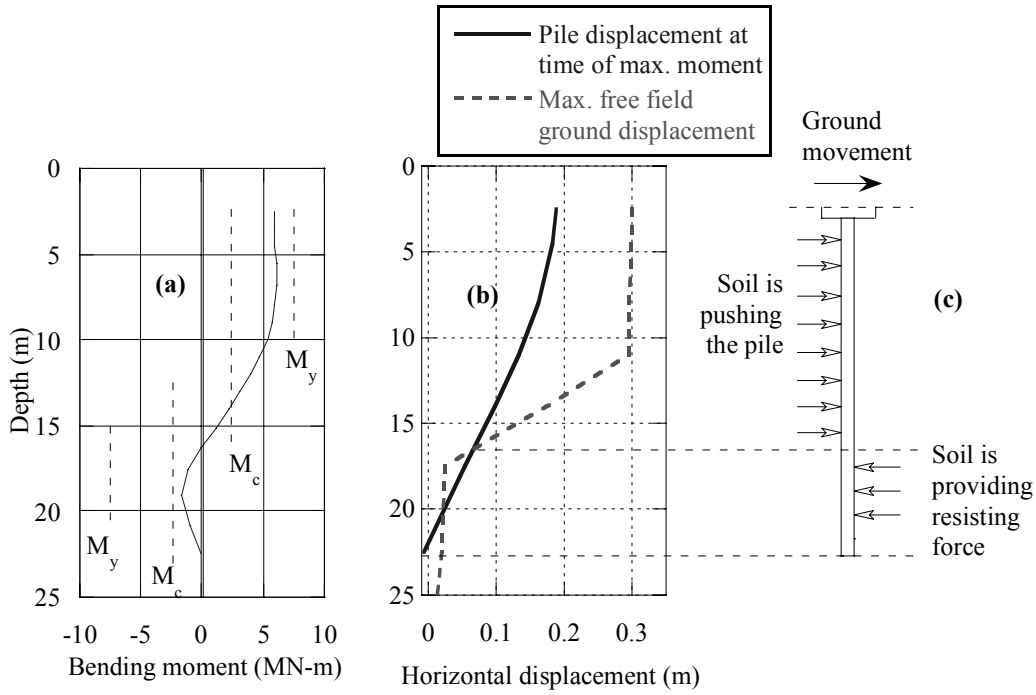

Figure 17. Computed pile response with non-linear base layer soil at the time of maximum moment: (a) pile bending moment distribution, (b) pile displacement profile compared to maximum free field ground displacement.

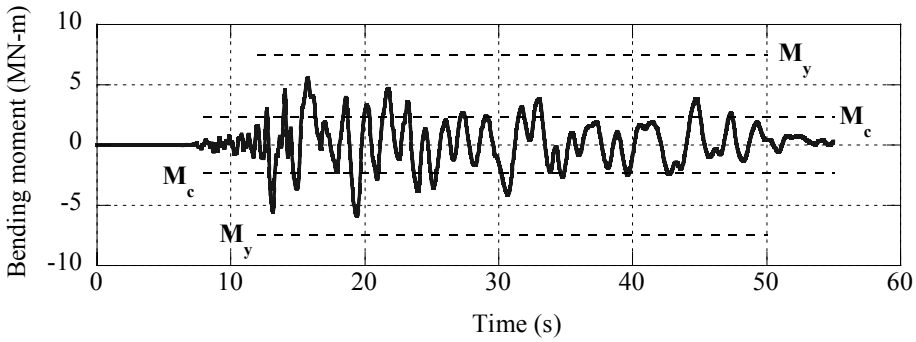

Figure 18. Bending moment time history at the pile head calculated using the non-linear base layer model.

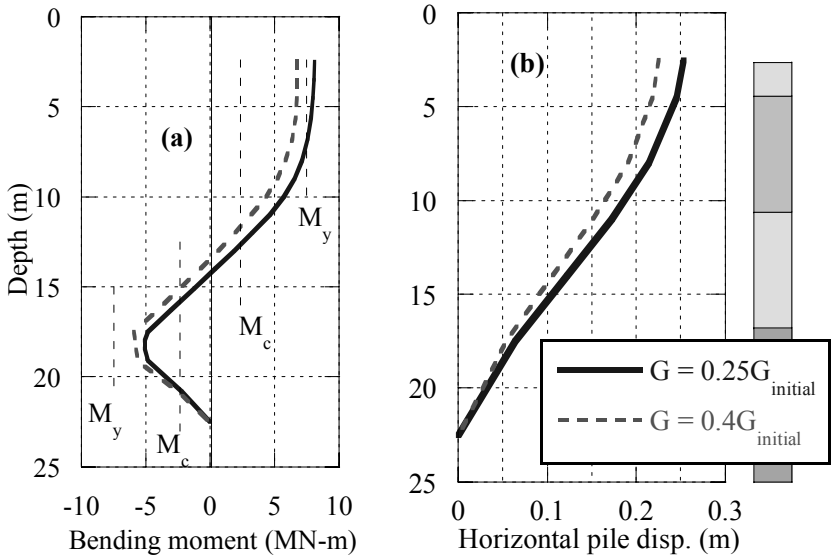

Figure 19. Computed pile response using equivalent linear base layer soil: (a) Maximum pile bending moment, (b) pile displacement profile at the time of the maximum moment.

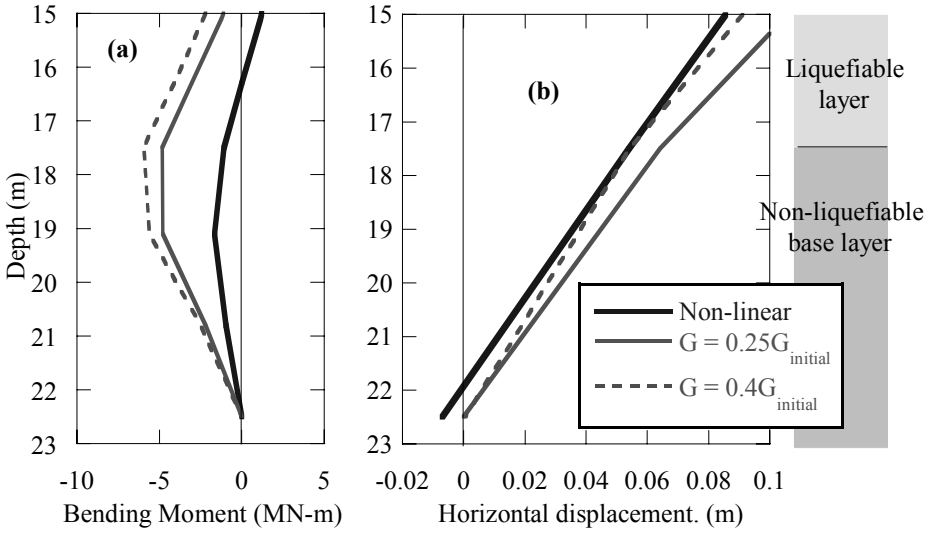

Figure 20. Computed pile response in the base layer (a) Maximum pile bending moment, (b) pile displacement profile at the time of the maximum moment.

Performance Levels

The preliminary design of the new piles was conducted following the Transit Bridge Manual, which refers the designer to the earthquake loadings code NZS 1170.5. With regard to the high importance level of the bridge, the code requires that two serviceability limit states and an ultimate limit state must be considered. These states correspond to events with annual probabilities of exceedance of 1/25, 1/500 and 1/2500 years respectively. Using NZS 1170.5 the design peak ground accelerations for these cases were determined as 0.06g, 0.25g and 0.44g. The strengthened foundation was designed to achieve certain performance levels for each case; these are given in Table 3.

With this in mind, three analyses were conducted to assess the performance of the central pier in the three earthquake events mentioned above. In these analyses, the numerical model with a nonlinear base layer was subjected to the base input motion shown in Figure 7 scaled to a peak acceleration of 0.06g, 0.25g and 0.44g respectively. Figure 21 shows the results of the three analysis cases where it can be seen that both the ground and pile responses are very small for the SLS1 case, and that the pile bending moment is well below the cracking moment. The SLS2 and ULS cases have much larger ground displacements and bending moments however in both cases the bending moment does not reach the yield level, indicating that the new piles of the central pier satisfy the performance objectives identified in Table 3. These analyses illustrate some of the benefits from the use of the effective stress analysis in the assessment of seismic performance of important structures, at different levels of ground motion intensity. A unique contribution in this assessment is that the seismic response is evaluated through a rigorous analysis considering the effects of pore pressures and liquefaction on the complex soil-structure interaction and dynamic response of piles.

Table 3 Design performance criteria for serviceability and ultimate states

Case	Event	PGA (g)	Desired performance
SLS1	1/25yr	0.06	Minor, easily repairable damage, no traffic disruption
SLS2	1/500yr	0.25	Bridge passable for emergency services only, yielding of piles OK. Significant repairs needed before bridge reopens.
ULS	1/2500yr	0.44	With some repairs bridge is passable for emergency services, piles may approach ultimate capacity. Replacement might be necessary for long term.

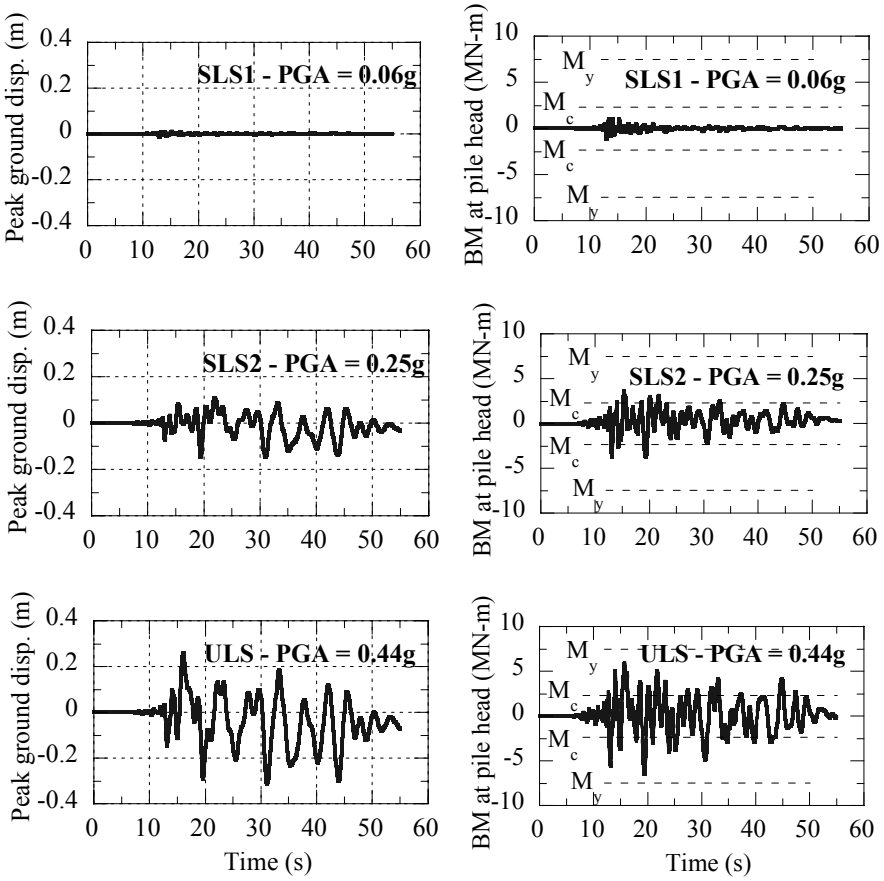

Figure 21. Time histories of peak ground displacement at the surface and bending moment at the pile head for three seismic cases corresponding to peak ground accelerations of 0.06g, 0.25g and 0.44g.

Comparison with Pseudo–static Analysis

It is interesting to compare the results of the effective stress analysis with those obtained using the conventional pseudo-static analysis of piles. In the latter approach, the complex dynamic forces are approximated by two static loads. Kinematic loads from the soil movement are applied to the pile as free-field ground displacements acting on a series of soil springs while inertial loads from the superstructure are modelled with a lateral force applied to the pile head. The stiffness of the soil springs, ultimate pressure from the soil and the free field ground displacement in this analysis are calculated using conventional empirical expressions such as those based on the SPT blow count. The pseudo-static analysis aims at estimating the maximum response of the pile, and this is done separately for the cyclic phase (during development of liquefaction) and lateral spreading phase (post-liquefaction phase). A detailed assessment of the pile foundation of Fitzgerald Avenue Bridges using the pseudo-static analysis is described in Bowen and Cubrinovski (2008).

Figure 22 compares the free field ground response computed with the effective stress analysis with that computed using a simplified empirical method that can be used in conjunction with the pseudo-static analysis. In Figure 22a, the maximum cyclic shear strains computed in the effective stress analysis are compared to the corresponding strains estimated from an empirical correlation based on the SPT blow count and the cyclic stress ratio (Tokimatsu and Asaka, 1998) using the soil profile in Figure 3. The shear strain in the surface layer from z = 2.5 to 4.5 m was limited to γ_{cyc} = 2%, as it was considered unlikely that strains larger than this will occur near the ground surface. By integrating the maximum shear strains throughout the depth of the soil profile, one can estimate the maximum lateral displacement of the ground, as shown with the broken line in Figure 22b. This lateral displacement is then applied to the soil springs as an input in the pseudo-static analysis of the pile. Figure 22b shows that in the case of the Fitzgerald Bridge analyses the simplified approach yielded a conservative result predicting a much larger lateral displacement of the ground in the shallow part of the deposit as compared to the seismic effective stress analysis. In the effective stress analysis, large strains occur only in the mid liquefied layer with N_1 =10, which is in accordance with the characteristics of the pore pressure generation and development of liquefaction, described in the previous section. The simplified procedure was unable to capture these complex characteristics of the ground response.

Due to the uncertainty regarding the stiffness of liquefied soils, two pseudo-static analyses were performed using different stiffness for the liquefied soil, with a degradation factor of 1/20 and 1/50 respectively. Both analyses used an inertial load corresponding to 0.44g ground acceleration.

The pile behaviour predicted by both pseudo-static analyses (dashed lines) and the effective stress analyses (solid lines representing the two equivalent linear cases) is compared in Figure 23. The maximum bending moment distributions are compared in Figure 23a where it can be seen that the distribution predicted by the effective stress analysis is similar to the pseudo static results. The bending moment at the interface between the liquefied and base soil layers is slightly lower, and the bending moment flattens out above the mid liquefied layer. In the pseudo-static analysis, the base layer is much stiffer and this results in a larger contrast in the stiffness between the liquefied layer and base layer, and hence higher interface bending moments.

Figure 23b shows that the pile displacement profile is different between the two methods. The pile is less constrained at the base in the effective stress analysis, due to the different modelling of the base layer as described previously. The displacement at the pile head predicted by the pseudo static analysis varies considerably as the stiffness of the liquefied soil is varied. The more rigorous effective stress analysis predicts a displacement in between the upper and lower bounds predicted in the simplified analysis. By and large, the results of the effective stress analysis and pseudo-static analysis are in good agreement and consistent with the assumptions made and details of modelling.

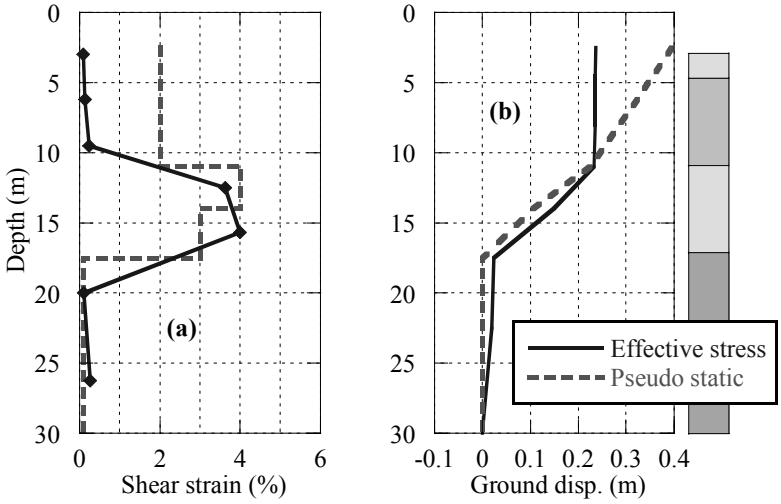

Figure 22. Comparison between the free field ground response calculated from the effective stress and pseudo static methods; (a) maximum cyclic shear strain, (b) ground displacement.

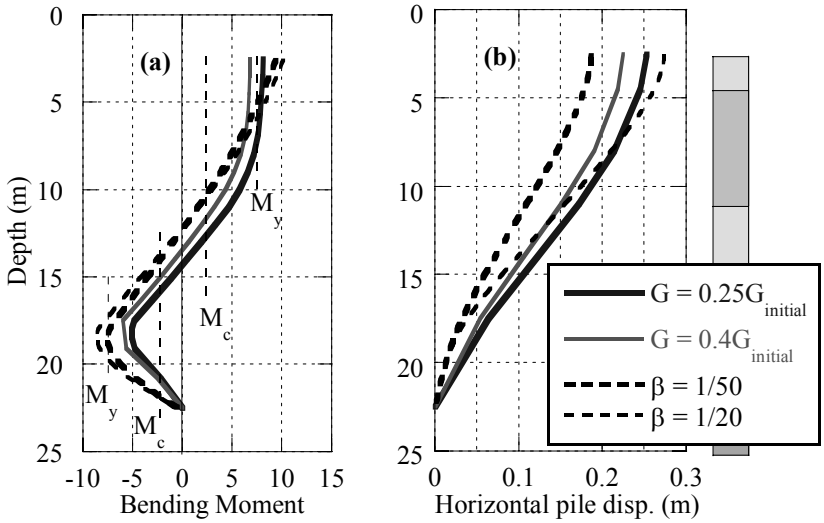

Figure 23. Comparison of pile behaviour between the two methods; (a) maximum bending moment distribution. (b) maximum pile displacement.

CONCLUSIONS

An advanced dynamic analysis based on the effective stress principle has been performed to evaluate the seismic performance of foundation piles of a bridge pier founded in liquefiable soils. This case study demonstrated the capability of the effective stress analysis to capture important features of the complex soil-pile interaction in liquefying soils including:

- Detailed development of excess pore water pressure through time and space including effects of soil density and complex interaction between intensity of shaking, pore pressures and associated ground deformation. Typical effects of liquefaction on the ground motion such as loss of high-frequency content and elongation of the period were also observed.
- The soil-pile interaction significantly affected both the response of the foundation soil and piles. The presence of piles increased the stiffness of the foundation soil and consequently reduced its deformability as compared to the free field ground. The peak ground displacements were about 18 cm and 28 cm in the soil in-between piles and the free field soil respectively.
- The seismic performance of piles was rigorously evaluated by taking into account the highly complex dynamic nature of loads and soil-pile interaction. The horizontal displacement of the piles reached about 18 cm to 25 cm and bending moments reached yield level at the top of the pile. Hence, the analysis provided very detailed information on the performance of the piles including development, variation and duration of loads and consequent damage level to piles.

For the above reasons, the advanced effective stress analysis is suitable for a rigorous evaluation of the seismic performance of pile foundations of important structures. It can explain complex features of the response and verify design assumptions, and hence, it provides a unique contribution in the assessment and design of piles.

ACKNOWLEDGEMENTS

Financial assistance from the New Zealand Earthquake Commission is gratefully acknowledged.

REFERENCES

Biot, M. A. Theory of propagation of elastic waves in a fluid-saturated porous solid, Part I – low frequency range; Part II – higher frequency range. (1956) *Journal of Acoustics Society of America*; **28**, 168-191.

Bowen, H. and Cubrinovski, M. (2008). "Pseudo-static analysis of piles in liquefied soils: a case study of a bridge foundation" *Bulletin of the New Zealand Society for Earthquake Engineering*, **41**(4), 234-246.

Cubrinovski, M., Ishihara, K. and Higuchi, Y. (1995). "Verification of a constitutive model for sand by seismic centrifuge tests." IS-Tokyo '95 First Int. Conference on Earthquake Geotechnical Engineering. Tokyo 1995; (2), 669-674.

Cubrinovski, M., Ishihara, K. and Tanizawa. (1996). "Numerical simulation of Kobe Port Island liquefaction." *11th World Conference on Earthquake Engineering*, Acapulco, Mexico (Paper No. 330).

Cubrinovski, M. and Ishihara, K. (1998a). "State concept and modified elastoplasticity for sand modelling." *Soils and Foundations*, **38**(4), 213-225.

Cubrinovski, M. and Ishihara, K. (1998b). "Modelling of sand behaviour based on state concept." *Soils and Foundations*, **38**(3), 115-127.

Cubrinovski, M., Ishihara, K. and Furukawazono, K. (1999). "Analysis of full-scale tests on piles in deposits subjected to liquefaction." *Second International Conference on Earthquake Geotechnical Engineering*, Lisboa 1999, 567-572.

Cubrinovski, M., Ishihara, K. and Furukawazono, K. (2000). "Analysis of two case histories on liquefaction of reclaimed deposits." Proc. 12th World Conference on Earthquake Engineering. Auckland 2000; CD-ROM, 1618/5.

Cubrinovski, M., Ishihara, K. and Kijima, T. (2001). "Effects of liquefaction on seismic response of a storage tank on pile foundations." *Fourth International Conference on Recent Advances in Geotechnical Earthquake*

Engineering and Soil Dynamics. San Diego 2001; CD-ROM, 6.15.

Cubrinovski, M., Uzuoka, R., Sugita H., Tokimatsu K., Sato M., Tsukamoto, Y., Ishihara, K., Kamata, T. (2008). "Prediction of pile response to lateral spreading by 3-D soil-water coupled dynamic analysis: shaking in the direction of ground flow", *Soil Dynamics and Earthquake Engineering*, *Elsevier*, Vol. **28** (6), 421-435.

Howard, M., Nicol, A., Campbell, L. and Pettinga, J. (2005). "Holocene paleoearthquakes on the strike-slip Porters Pass Fault, Canterbury, New Zealand." *New Zealand Journal of Geology and Geophysics*, **48**, 59-74.

Ishihara, K. and Cubrinovski, M. (2005). "Characteristics of Ground Motion in Liquefied Deposits During Earthquakes", *Journal of Earthquake Engineering*, **9**(1), 1-15.

Pettinga, J., Yetton, M., Van Dissen, R. J. and Downes, G. (2001). "Earthquake source identification and characteristation for the Canterbury Region, South Island, New Zealand." *Bulletin of the New Zealand Society for Earthquake Engineering*, **34**(4), 282-316.

Stirling, M., Pettinga, J., Berryman, K. and Yetton, M. (2001). "Probabilistic seismic hazard assessment of the Canterbury region, New Zealand." *Bulletin of the New Zealand Society for Earthquake Engineering*, **34**(4), 318-334.

Tokimatsu, K. and Asaka, Y. (1998). "Effects of liquefaction induced ground displacements on pile performance in the 1995 Hyogoken-Nambu Earthquake." *Soils and Foundations* (Special Issue), 163-177.

Youd, T. L., Idriss, I. M., Andrus, R. D., Arango, I., Castro, G., Christian, J. T., Dobry, R., Liam Finn, W. D., Harder L.F, Jr., Hynes, M. E., Ishihara, K., Koester, J. P., Liao, S. S. C., Marcuson III, W. F., Martin, G. R., Mitchell, J. K., Moriwaki, Y., Power, M. S., Robertson, P. K., Seed, R. B. and Stokoe Ii, K. H. (2001). "Liquefaction resistance of soils: Summary report from the 1996 NCEER and 1998 NCEER/NSF workshops on evaluation of liquefaction resistance of soils." *Journal of Geotechnical and Geoenvironmental Engineering*, **127**(10), 817-833.

Zienkiewicz, O. C. and Shiomi, T. (1984). "Dynamic Behaviour of Saturated Porous Media: the Generalised Biot Formulation and its Numerical Solution." *International Journal for Numerical and Analytical Methods in Geomechanics*, **8**(1), 71-96.